

URTeC 1581308

Estimation of Dispersion in Orientations of Natural Fractures from Seismic Data: Application to Discrete Fracture Network Modeling

Reinaldo J. Michelena*, Kevin S. Godbey, Huabing Wang, and James R. Gilman, iReservoir.com, Inc.;
Chris K. Zahm, Bureau of Economic Geology, University of Texas at Austin

Copyright 2013, Unconventional Resources Technology Conference (URTeC)

This paper was prepared for presentation at the Unconventional Resources Technology Conference held in Denver, Colorado, USA, 12-14 August 2013.

The URTeC Technical Program Committee accepted this presentation on the basis of information contained in an abstract submitted by the author(s). The contents of this paper have not been reviewed by URTeC and URTeC does not warrant the accuracy, reliability, or timeliness of any information herein. All information is the responsibility of, and, is subject to corrections by the author(s). Any person or entity that relies on any information obtained from this paper does so at their own risk. The information herein does not necessarily reflect any position of URTeC. Any reproduction, distribution, or storage of any part of this paper without the written consent of URTeC is prohibited.

Summary

This paper describes a statistical methodology to estimate dominant fracture orientation and dispersion from seismically-calculated 3D structural attributes. The dispersion parameter, the circular variance, can be easily associated with the Fisher coefficient, a key parameter in the probability density function used in discrete fracture network modeling to stochastically generate fracture orientations. We show examples of applications to seismic constrained DFN modeling and perform flow simulations on fractured models built using different dispersion parameter models to discuss possible implications for drainage of naturally fractured, unconventional reservoirs.

Introduction

The design of horizontal wells and hydraulic fracture stimulation requires a detailed understanding of the variations in relative orientations of natural fractures and local stress field across the reservoir. Structural attributes extracted from poststack 3D seismic data such as curvature, semblance or dip, have been used in the estimation of preferential orientation in the subsurface, in particular orientation of natural fractures. Attributes derived from the analysis of prestack amplitude variations vs. offset and azimuth (AVOZ) have also been used for this purpose (Rüger, 2002). After careful calibration with log derived fracture orientations, orientations derived from seismic data may be used as a proxy for orientations of the natural fractures. However, these orientations may be misleading or difficult to interpret when multiple fracture orientations are present.

The model-based nature of AVOZ analyses (which assume either a single set of vertical fractures, two sets of orthogonal vertical fractures or any of the above with a tilted axis of symmetry) may yield uncertain results when the assumptions of the fracture model are not met. In many geological settings, several non-orthogonal fracture sets occur with different dips and azimuths that overlap in the same volume of rock. Approaches that use poststack data and overcome the model-based limitations of using prestack data typically yield a single orientation per sample with no indication of how to interpret it when multiple orientations are present. Chopra et al. (2009), however, do go beyond single-orientation answers. The authors generate what they refer to as “3D rose diagrams” volumes after analyzing orientations of the azimuth of minimum curvature for each horizontal time slice. Even though their rose diagrams provide a visual idea of the dispersion in fracture orientation, no quantitative estimates of this dispersion are generated. Furthermore, rose diagrams based on 2D time slices fall short in capturing the real 3D nature of the fracture orientation that requires two parameters (dip and dip-azimuth) instead of only one used to generate rose diagrams (dip-azimuth).

Natural fracture orientations and intensities derived from seismic data can be used to constrain discrete fracture network (DFN) modeling as long as careful calibration of the seismic attribute with local well data is performed to test that the attribute carries information about actual natural fractures (e.g., Will et al., 2005). More information besides average orientation is required to construct a stochastically generated DFN model. Fracture orientations also require a parameter called the Fisher coefficient that measures the dispersion in fracture directions (Mardia, 1972). A high Fisher coefficient is related to fractures aligned primarily in one orientation, whereas a low value indicates fractures with many orientations. Even though the Fisher coefficient is 3D in nature, it is usually estimated from 1D image log data which record fracture dip and dip-azimuth. The average orientation and degree of dispersion is estimated along the well and assumed to be constant in the interwell region in DFN modeling applications. Because of this assumption, local orientations of modeled fractures will have the same dispersion as those at the wells, a hypothesis that may not necessarily be valid, implying that estimates of 3D variability in orientation dispersion from seismic data are needed.

We propose a methodology to estimate dominant orientations and orientation dispersion from structural seismic attributes that can be used to constrain DFN models. First, we start by extracting dip and dip-azimuth information from the chosen structural attribute and compare the results with orientations derived from image log data. Since orientations may vary significantly within small areas, we extract a more consistent and less noisy dominant orientation and capture the dispersion in the orientations by estimating a quantity that generalizes the concept of circular variance, is independent of the direction of the reference axis for angles, and can be easily transformed into the Fisher coefficient used for DFN modeling. We elaborate on the meaning of this dispersion and explain how to estimate it from seismic data. Then, we show how to use dominant orientation and dispersion volumes to constrain DFN modeling. The value of the approach is demonstrated with a simple DFN modeling example that incorporates fracture intensity, dominant orientation and orientation dispersion from seismic data into the modeled fractures. Finally, we build simple flow simulation models using parameters typical of unconventional reservoirs to illustrate the importance of fracture dispersion in the drainage of unconventional reservoirs.

Orientations from structural attributes

Once the interpreter selects the attribute(s) that best respond to faulting and possible natural fractures, we need to estimate orientations from these attribute(s) that can be related to local fault planes. We use the local 3D gradient of the attribute to achieve this goal. The calculation of the gradient in 3D also requires velocity information or a structural attribute volume in depth domain if meaningful estimates of the real dip are to be extracted, analyzed, and calibrated with well information. The plane perpendicular to the 3D gradient at each point in the volume can be interpreted as a local fault plane.

Figure 1a shows the intersection of local fault planes with a stratigraphic horizon which result in the blue segments parallel to local fault strikes. The attribute represented in this figure is the maximum curvature. Notice how variable local strikes can be in particular within fault anomalies. Even though these local orientations may look like “noise” in some areas, we will show that they contain valuable information about the possible dispersion in subseismic fracture orientations. The following section describes how to estimate this dispersion.

Statistics of seismic derived orientations

As we discussed in the previous section, local fault orientations estimated from the 3D gradient may look noisy and even unreasonable in some areas. Due to a variety of reasons that range from data quality issues and resolution to structural complexity, local strikes estimated from the gradient are not necessarily reliable on a “point-by-point” basis. However, we propose that when analyzed collectively in a statistical fashion, these “noisy” orientations may reveal important information about dispersion in subseismic fracture orientation across the reservoir.

Calibration with log data. Before using seismic derived orientations to help map orientation of natural fractures, we should first make sure that these orientations are indeed related in the area of interest. Figure 1b shows an example of differences between dip-azimuth orientations estimated from maximum curvature and from image logs. In this figure, dip-azimuth orientations estimated from seismic data have been extracted along the well paths where discrete fracture interpretations from image logs are also available. Due to the large difference in resolution between seismic and image log information (seismic attribute in the order of tens of meters vs. individual fractures from image logs in the order of a few centimeters) we don't expect a point-by-point agreement between both orientations along the

well paths. However, image log and seismic derived orientations do show a good statistical agreement when compared across the whole reservoir interval. The good agreement between these two rose diagrams shows that seismic derived angles may be a reasonable proxy to estimate dominant fracture orientations in the interwell region. If these two rose diagrams were not in approximate agreement, we should question whether seismic derived orientations can be used to help map fracture orientation in the area.

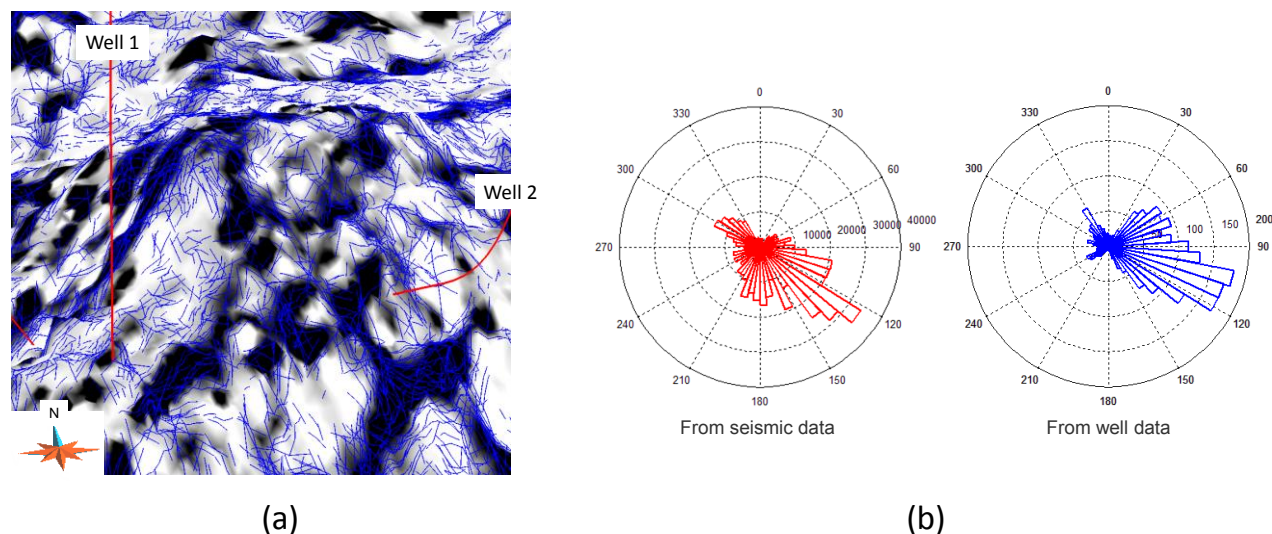


Figure 1. (a) Local strike orientations (blue lines) overlaid on the maximum curvature attribute extracted along a stratigraphic horizon. Blue strike lines are centered in a 25m x 25m cell size surface. Only strikes related to the largest gradients are shown. The statistical analysis of these apparently “noisy” orientations contains important information about the dispersion in fracture orientation in the reservoir. (b) Rose diagrams of dip-azimuth (perpendicular to strike) orientations from fractures interpreted in image logs and seismic derived dip-azimuth angles from local gradients of maximum curvature projected along the same well path where image logs are available. General orientation trends from seismic and well data are very similar which confirms that orientations derived from seismic data can be used to estimate fracture orientations. In these rose diagrams, zero degrees correspond to the North.

Mean or dominant fracture orientation? In order to understand the variability in fracture orientation across the area of interest, we can extract different statistical measures from angles within small blocks of cells in the larger 3D volume and these results are assigned back to the center of the block in a moving average fashion. For instance, we can compute local histograms of angles (rose diagrams) as proposed by Chopra et al. (2009) to analyze the variability in dip-azimuth. We can also extract polar plots to analyze the real 3D nature of the fracture orientation that requires dip and dip-azimuth angles.

The simplest measure we can extract from a set of angles in a given subvolume is the average. This measure, however, can be misleading because circular variables like the angles cannot always be averaged as if they were linear variables. Even if we do the angle average properly by averaging the unit vectors that correspond to each orientation, the result can still be misleading because we may end up with average orientations that have nothing to do with the orientations actually observed in the field. For instance, if two dominant fracture orientations at 0 and 90 degrees respectively are observed in the reservoir, an average orientation of 45 degrees is meaningless from the fluid flow point of view. A measure that does not suffer from these limitations is the mode of the histogram, or dominant fault orientation. We think that the mode is a more sensible estimate of an “equivalent” angle in a block where multiple orientations are present.

Figure 2a shows the maximum curvature extracted along a stratigraphic horizon along with small segments indicating the local strike orientations derived from the gradient and projected along the horizon (Figure 2b). Notice how the dominant angles (Figure 2c) are less noisy and more consistent across the area. Figure 3 shows the rose diagrams for the different areas highlighted in Figure 2. Areas (a) and (b) show similar fracture strike orientation with the difference that in area (b) most fractures dip towards the SE whereas in area (a) fractures dip towards both

NE and SW. Fractures in region (c) are oriented in many directions. Most dips in the area (not shown) are between 60 and 80 degrees.

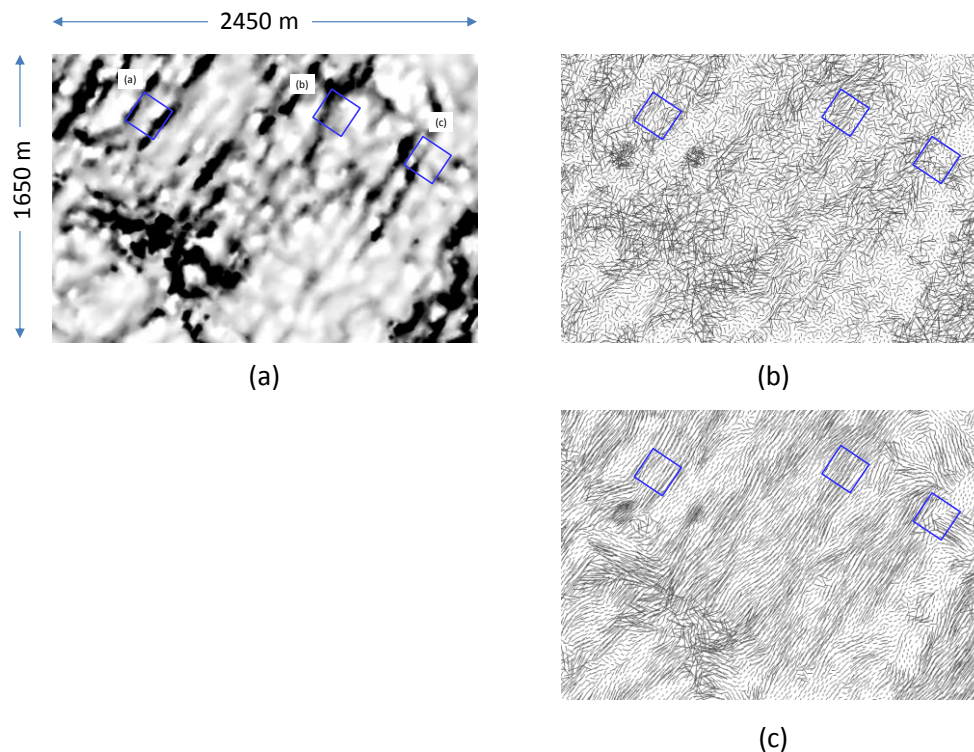


Figure 2. (a) Maximum curvature with areas of interest (in blue). (b) Original local fault strikes estimated by using the gradient of the maximum curvature. (c) Dominant orientations (mode) extracted from moving blocks of $200\text{ m} \times 200\text{ m} \times 20\text{ m}$ and assigned to the center of each block. Dominant orientations are more consistent and less noisy than original orientations. The length of the segments is proportional to the magnitudes of the local gradient typically related to stronger anomalies. Areas indicated by blue squares will be analyzed in detail in subsequent figures.

Dispersion in fracture orientation. In linear statistics where a single number such as the mean or mode is insufficient to describe the shape or distribution of a set of numbers and higher moments such as the variance are also needed, in circular statistics we can also estimate a circular variance V as follows (Fisher, 1995):

$$V = 1 - R/N, \quad (1)$$

where N is the total number of angles used for the analysis and R is the magnitude of the vector sum of all unit vectors related to each direction. Unlike the linear variance that can take any positive value, the circular variance varies between 0 (all unit vectors pointing in the same direction) and 1 (all unit vectors pointing in directions that cancel each other).

The probability density function used in DFN modeling to stochastically generate subseismic fracture orientations also requires a parameter called the Fisher coefficient that measures the dispersion in fracture directions (Mardia, 1972). The Fisher coefficient (K) is defined as $K = 1/V$ and ranges between 1 and infinity. A high Fisher coefficient is related to fractures oriented primarily around one orientation, whereas a low value indicates fractures in many orientations.

The estimation of a Fisher coefficient suitable for describing fracture orientations from the circular variance, however, is not straightforward because the circular variance is designed to measure the spread in directions, not orientations. Since fracture planes have orientation but their dip dependent direction is irrelevant to describe the relationship of their strike with respect to some reference axis in the horizontal plane, the Fisher coefficient estimated from the circular variance may not be totally adequate to describe variability in fracture orientations and

may yield artificially low values in areas like (a) (see Figure 2 and Figure 3) where fractures show the same orientation but opposite directions that correspond to opposite dip directions. Eliminating the direction component by referring all angles to the range $[0,180)$ degrees does help to alleviate this problem but does not solve it along whatever axis is chosen as a reference.

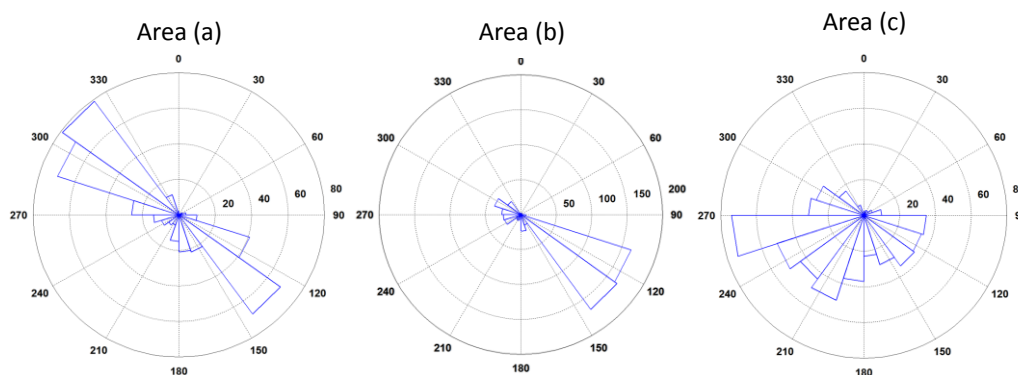


Figure 3. Dip-azimuth rose diagrams (below) for the different areas highlighted in Figure 2. Area (a) shows dips towards the NW and SE and area (b) shows dip predominantly towards the SE. Areas (a) and (b) show that most dip-azimuths are clustered around the same angles whereas area (c) shows more dispersion.

Let's examine this problem by analyzing in detail the estimation R/N in the simple example shown in Figure 4. Figure 4a shows all unit vectors in the upper part of the figure plotted from the same origin and referring the angles to the North. Since all angles fall in the range $[0,180)$, there is no need to subtract 180 from the original angles and the average magnitude of the sum of all unit vectors R/N is 0.9882 (out of a maximum of 1 if all unit vectors were identical). Figure 4b shows the same unit vectors but now referring the angles to the East. When we choose this origin, we obtain some angles greater than 180 degrees and therefore, we need to refer some angles back to the interval $[0,180)$. The result is shown in Figure 4c. Even though fracture orientations in Figure 4b and Figure 4c are the same, the average magnitude R/N in Figure 4c is 0.6863, erroneously suggesting a larger dispersion than in Figure 4a that represents identical fracture orientations. The reason for this apparent "error" is that orientations near the selected axis of reference for the angles may result in an artificially low sum of unit vectors if they point in nearly opposite directions.

Only in two cases is the dispersion independent of the selection of the reference axis: a) when all orientations are identical; or b) when the dispersion is the highest and fractures are randomly oriented in the block of interest. All other intermediate cases that result in higher dispersion with respect to one axis will look lower with respect to another. As explained above, when all orientations are identical we obtain $R/N = 1$. In the opposite extreme, when fractures are randomly oriented (as in Figure 5a), it is easy to show that $R/N \approx 0.6366$, which is the average of the sine function in the interval $[0, \pi]$.

The examples of Figure 4 and Figure 5 show extreme cases in orientation dispersion from all fractures clustered around a single angle to fractures spread uniformly across all angles. As we have discussed, if we estimate the dispersion by averaging the magnitude of the sum of unit vectors, the result will depend on the selection of the reference axis because fracture orientations near the reference may produce artificially low sums. However, these apparently low values that indicate high dispersion may be re-estimated by using a reference axis that is orthogonal to the first axis. In other words, if we compute R/N for two orthogonal reference axes and we select the highest value from the two results, we ensure that fracture dispersion will not be overestimated because of the proximity of the orientations to a particular reference axis.

To summarize, the steps needed to estimate orientation dispersion M at a point are:

- 1) Select the first of the two reference axes needed.
- 2) Generate dip-azimuth direction angles with respect to this axis.
- 3) Refer all direction angles to $[0,180)$ degree range orientations.
- 4) Select a second reference axis orthogonal to the first one. Refer all angles to the new $[0, 180)$ degree range.
- 5) Compute R/N for each set of orientation angles and extract the maximum M .

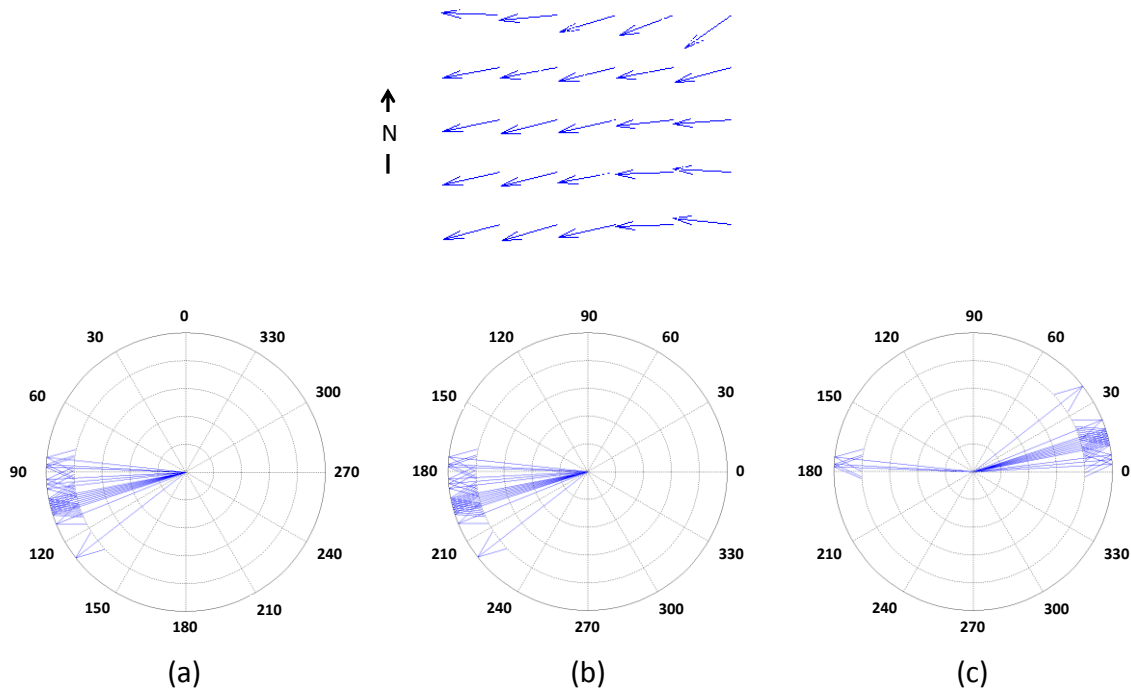


Figure 4. Above: Area with 25 predominantly EW fractures. Below: Unit vectors that correspond to the 25 strike orientations. (a) All angles are referred to the North. The average magnitude of the sum of all unit vectors in this case is 0.9882 (out of a maximum of 1 if all orientations were identical). (b) All angles are referred to the East. The sum of all unit vectors is the same as (a). (c) All angles are referred to the East but 180 degrees have been subtracted from orientations greater than 180. Cases (b) and (c) represent identical fracture orientations, although different directions may be related to the corresponding unit vectors. The average magnitude of the sum of all unit vectors in (c) is 0.6863 (less than the 0.9882 obtained in (a)) because directions along the EW axis tend to cancel each other.

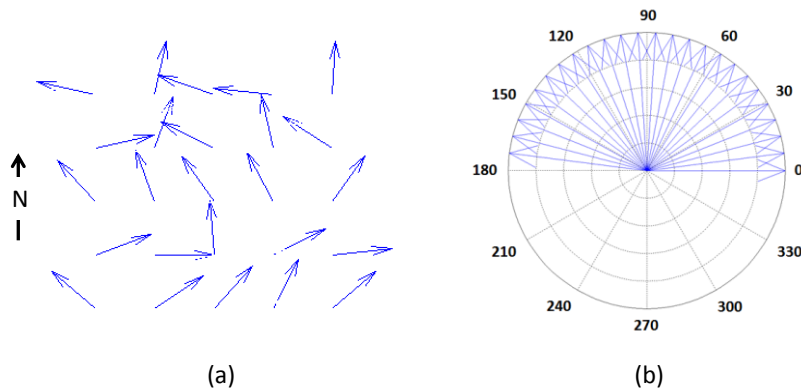


Figure 5. (a) Area with 25 random fracture orientations. (b) Random unit vectors referred to the interval $[0, 180)$ degrees. The average R/N of all 25 unit vectors in this case is 0.6358. For a continuum of random orientations the average R/N is $2/\pi$ (≈ 0.6366).

The estimate of dispersion M needs to be normalized between 0 and 1 before it can be transformed into the Fisher coefficient required for DFN modeling. The minimum of M occurs when the orientations in the block of interest are completely random which results, as we explained above, in $M = 2/\pi$ (a formal theoretical demonstration of this is beyond the scope of this paper but we will demonstrate it empirically in the field data example that follows). Based on this fact, is easy to show that the Fisher coefficient K can be calculated by using the following expression:

$$K = \frac{1 - 2/\pi}{1 - M}. \quad (2)$$

Figure 6 shows the result of the estimation of R/N for different reference axes (Figure 6b and Figure 6c) and the maximum of the two (Figure 6d). Areas of low R/N indicate high fracture orientation dispersion and areas of high R/N indicate areas where fracture orientations do not change significantly. Figure 7 shows a crossplot of the values of R/N estimated by referring the angles to the East and to the North. This crossplot is colored by the maximum of the two estimates. Notice how the minimum of R/N for each axis is approximately 0.6 which, as explained in Figure 5, corresponds to the case of randomly oriented fractures.

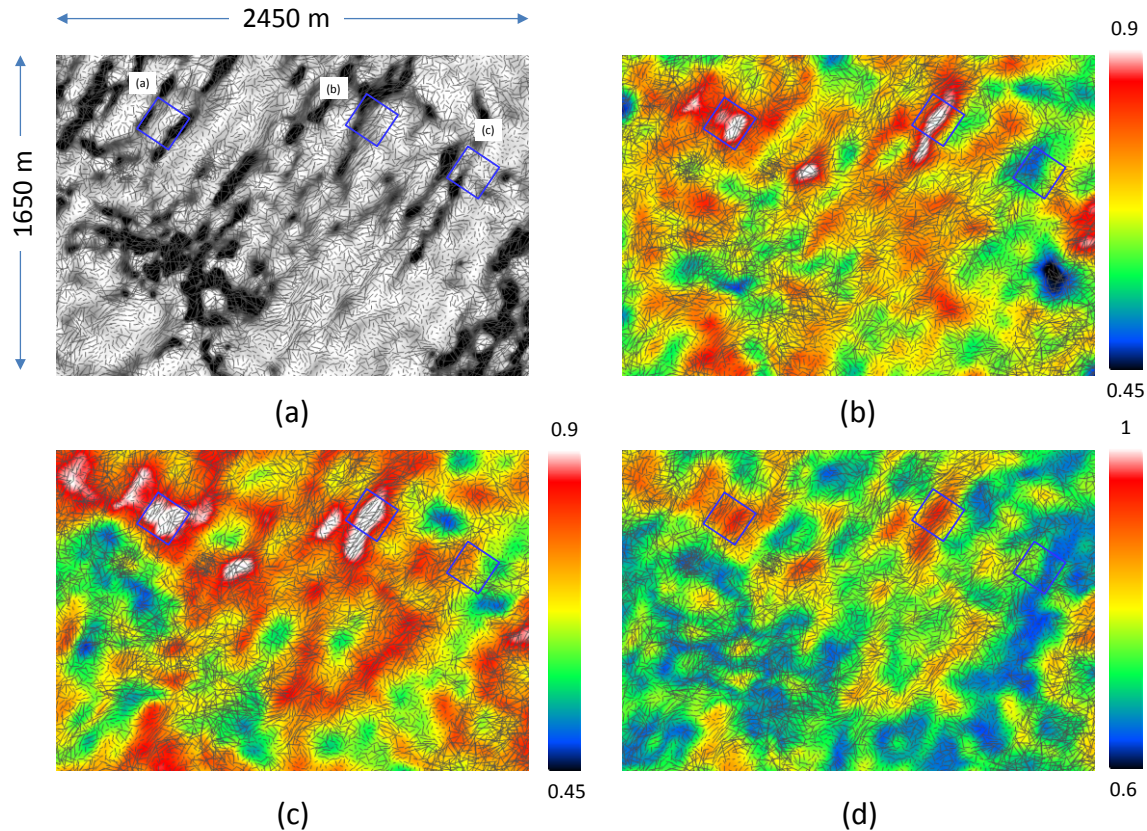


Figure 6. (a) Maximum curvature. (b) R/N estimated by referring all angles to the East. (c) R/N estimated by referring all angles to the North. (d) Maximum of maps (b) and (c) which can be transformed into the Fisher coefficient for DFN modeling. Original local fracture orientations are also shown in each figure for reference.

Application to DFN modeling

We built several discrete fracture models (DFM) using the methodology explained above assuming fractures of constant aperture, height and length. For this example, intensity (P32 or fracture area/unit volume) is assumed to be proportional to the maximum curvature (Figure 8a). Figure 8b shows the dominant fracture orientations extracted from gradients computed from the maximum curvature (same as Figure 2c). Figure 8c shows the Fisher coefficient derived from Figure 6d using equation 2 for the maximum circular variance. Figure 8d shows the intersection of the modeled fractures with the horizon of interest. Notice how local orientations in this DFM are determined by the dominant orientation and the local Fisher coefficient.

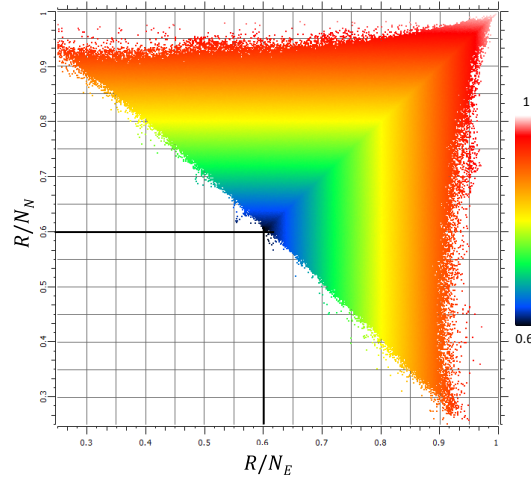


Figure 7. Crossplot of R/N estimated by referring all angles to the East (horizontal axis) and to the North (vertical axis). The color is the maximum of the two axes. Notice how the minimum of R/N for each axis occurs in the upper vicinity of 0.6, which, as explained in Figure 5, corresponds to the case of randomly oriented fractures.

To illustrate the effect of the Fisher coefficient on directional permeability, we also defined two alternative DFMs with a large Fisher coefficient (1000) uniformly assigned throughout the model area resulting in strong directional permeability anisotropy around the dominant orientation and, alternatively, with a small Fisher coefficient (1) uniformly assigned throughout the model area resulting in more isotropic permeability. There is still significant cell-to-cell permeability variation in both cases as defined by variability in fracture intensity. The average effective fracture permeability assumed for these DFMs is on the order of 0.5 md. The DFMs were then upscaled for dual-media flow simulation models (Dershowitz et al., 2000) assuming a matrix permeability on the order of that seen in commercial unconventional reservoirs (1 μ D) and were initialized with under-saturated oil on the order of 1cp viscosity. Both models were then run with a horizontal well (Figure 9) producing at a fixed bottom-hole pressure of 500 psia. Initial pressure is 6750 psia. Along the horizontal wellbore, five times permeability enhancement (representing multistage hydraulic fracturing with 150 ft effective stimulated radius) is applied in the model. Figure 9a shows that reasonable unconventional well initial production (IP) rates have been achieved through this near wellbore permeability enhancement approach.

Figure 9a also shows the decline behavior for the simulations showing expected decline behavior for unconventional reservoirs. However, both models show minimal rate differences which demonstrate that decline behavior alone cannot distinguish the nature of the pressure depletion in the reservoir. Figure 10b compares the pressure difference for the two uniform Fisher coefficient models after 100 days of simulation. The map is shaded according to pressure difference of the two models. Blue colors represent the case where the large uniform Fisher coefficient (1000) results in lower pressure than the small Fisher coefficient (1). Red represents the reverse situation. The trends in the blue shading show that when open fracturing is intense and highly directional (large permeability anisotropy), the pressure depletion is more localized to the areas of high fracture intensity. In the case with a low Fisher coefficient, the pressure wave will move more slowly away from the well in these highly fractured areas resulting in more uniform depletion all along the well as shown by the red coloring even in lower intensity areas.

The impact of stress on the permeability on individual fractures has not been incorporated in this simulation study and it is expected that favorably oriented fractures are more likely to be naturally open or to open under shear during hydraulic fracture operations. Calibration of the seismic interpretation to FMI, micro-seismic, hydraulic fracturing treatment pressures, well tests, offset well interference, and production decline, all within the confines of geomechanical constraints are required to better characterize the depletion behavior and optimize hydraulic fracture treatments and well spacing in naturally fractured unconventional reservoirs.

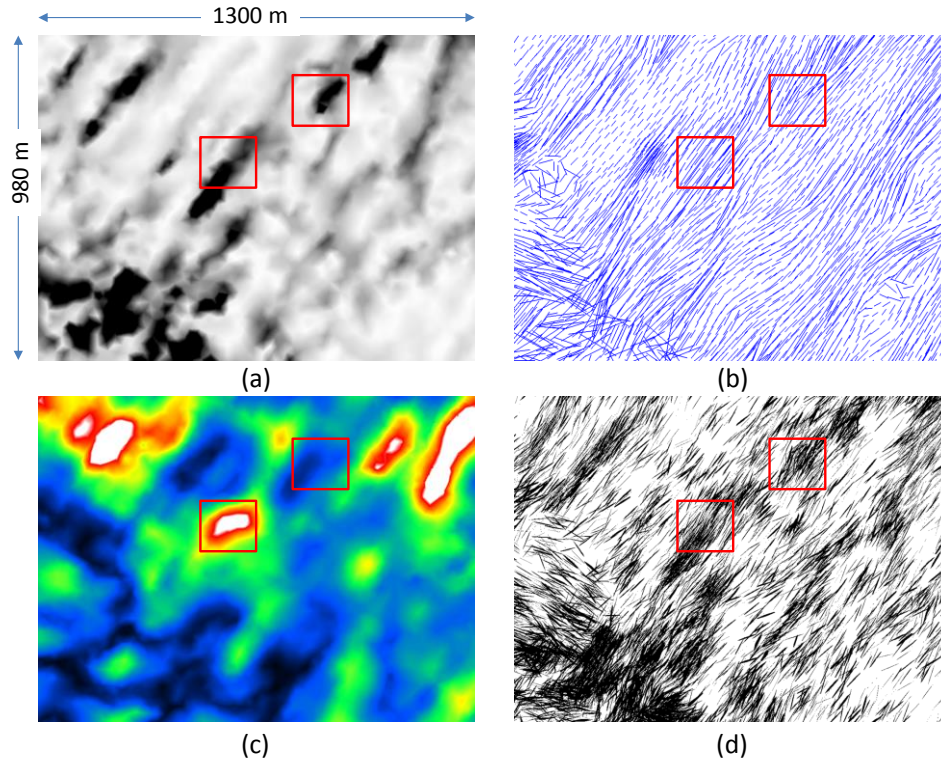


Figure 8. Seismic constrained DFN modeling over a portion of the area shown in Figure 6. (a) Original maximum curvature along stratigraphic horizon that is assumed to be proportional to fracture intensity. (b) Dominant orientation. (c) Fisher coefficient calculated from Figure 6d (from low-black to high-white values). (d) DFN modeled fractures that intersect the horizon of interest. Modeled fractures capture expected intensity, orientation and local dispersion extracted from the seismic data.

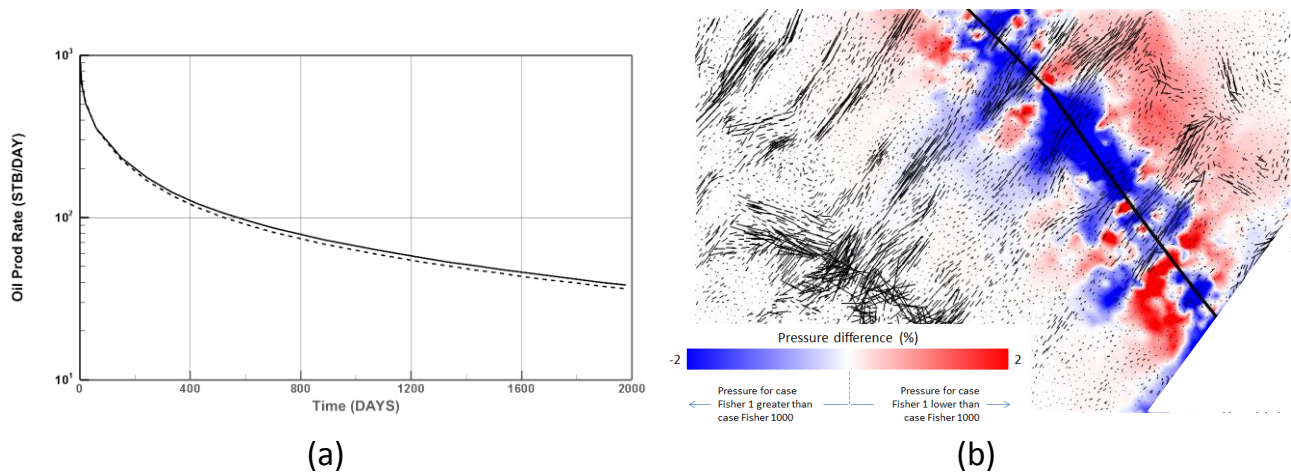


Figure 9. a) Decline behavior of two models with high (1000) and low (1) Fisher coefficient. Notice that rate difference is minimal which illustrates that decline behavior alone cannot distinguish the heterogeneous nature of the pressure depletion in the reservoir. b) Pressure difference between two uniform Fisher coefficient models after 100 days of simulation. Black, thick line indicates a horizontal well trajectory. Blue colors represent the case where the large uniform Fisher coefficient results in lower pressure than the small Fisher coefficient. Red represents the reverse situation. The trends in the blue shading show that when open fracturing is intense and highly anisotropic, the pressure depletion is more localized to the areas of high fracture intensity.

Downloaded 09/27/18 to 50.203.133.34. Redistribution subject to SEG license or copyright; see Terms of Use at http://library.seg.org/

Discussion and Conclusions

We have presented a methodology to estimate dominant fracture orientation and orientation dispersion from seismic data and to use this information to constrain DFN models. The estimation of dispersion (Fisher coefficient) is based on the maximum circular variance extracted from two orthogonal axes for the origin of angles.

We also show flow simulation examples in models built using very different dispersion conditions to assess the effect of dispersion in permeability anisotropy. These flow simulation models are built with parameters typical of an unconventional reservoir. The simulations show that fracture dispersion is expected to have significant implications on fluid flow behavior because of the impact on natural fracture permeability behavior prior to and subsequent to hydraulic fracturing treatments. For the cases illustrated here, high intensity fractured areas (fracture swarms) with large Fisher coefficients will result in significant pressure depletion pathways extending away from the wells and non-uniform pressure depletion along the well path. Although not illustrated here, non-uniform flow behavior will be even more severe during injection processes (e.g. miscible gas, surfactant or water).

Typically, as we mentioned in the introduction, the estimation of fracture orientation from AVOZ analysis assumes a single set of vertical fractures (Rüger, 2002). In terms of velocity anisotropy, this situation can be described by a horizontal transversely isotropic model (HTI) which corresponds to the case of a very high Fisher coefficient. On the other extreme, a very low Fisher coefficient corresponds to fractures with many different orientations that from the wave propagation point of view behave like an isotropic model. Velocity anisotropy models for situations that require symmetries more complex than HTI (from orthorhombic to triclinic) will result in intermediate Fisher coefficients but the actual correspondence between them (if any) requires further research.

References

- Chopra, S., Marfurt, K.J., and Mai, H.T., 2009, Using automatically generated 3D rose diagrams for correlation of seismic fracture lineaments with similar lineaments from attributes and well log data: *First Break*, **27**, 37-42.
- Dershowitz, W., LaPointe, P., Eiben, T., and Wei, L., 2000, Integration of discrete fracture network methods with conventional simulator approaches: *Society of Petroleum Engineers Res. Eval. & Eng.*, 165-170.
- Fisher, N.I., 1995, *Statistical analysis of circular data*: Cambridge University Press.
- Mardia, K.V., 1972, *Statistics of directional data*: Academic Press.
- Oda, M., 1985, Permeability tensor for discontinuous rock masses: *Geotechniques*, **35**, 483-495.
- Rüger, A., 2002, Reflection coefficients and azimuthal AVO analysis in anisotropic media: *Geophysical Monograph Series*, **10**, Society of Exploration Geophysicists.
- Will, R., Archer, R., and Dershowitz, W.S., 2005, Integration of seismic anisotropy and reservoir-performance data for characterization of naturally fractured reservoirs using discrete-feature-network models: *Society of Petroleum Engineers*, SPE-84412-PA.